Fizika Nizkikh Temperatur, 2006, v. 32, No. 11, p. 1330–1344

# Aspects of hole-burning and spectro-temporal holography in molecular doped solids

**(Review Article)**

Jean-Pierre Galaup

*Laboratoire Aimé Cotton, CNRS UPR 3321 & Université Paris XI,*
*Bât. 505, 91405 Orsay cedex, France*
E-mail:jean-pierre.galaup@lac.u-psud.fr

Received March 15, 2006

The persistent spectral hole-burning (PSHB) phenomenon is known since 1974. It is still an important research area for the study of the intimacy of complex molecular systems in the solid state, revealing high resolution spectra, photophysics, photochemistry and dynamics of molecular doped amorphous media, organic as well as inorganic. From another point of view, PSHB allows the engraving of any spectral structures in the inhomogeneous absorption band profile of molecular doped amorphous hosts or ion doped crystals cooled down to liquid helium temperatures. Therefore, a PSHB material is programmable in the spectral domain and consequently it can be transformed in an optical processor capable to achieve user-defined optical functions. Some aspects of both fields are illustrated in the present paper. Concerning the search of efficient PSHB materials, the hole burning performances and the photophysics of polymer and xerogel based systems are compared. The problem of high-temperature persistent spectral hole-burning materials and the search for new frequency selective photosensitive systems for fast optical pulse processing at 800 nm are considered. Regarding the points treated, inorganic hosts based on silicate xerogels or porous glasses have shown the best results. Moreover, by combining inorganic and organic capabilities or by grafting organic species to the host, hybrid xerogels have not yet revealed all possibilities. Also, the interest of two-photon materials for engraving spectral features with near-infrared or infrared light is developed. As an introduction to possible applications of PSHB material, the basics of spectro-temporal holography are remembered and a demonstrative experiment using a naphthalocyanine doped polymer film is described, proving that the temporal aberration free re-compression of ultrashort light pulses is feasible, therefore opening a way for applications in ultrashort light pulse shaping. Aspects for a comparison between cw hole-burning and femtosecond spectro-temporal experiments are considered and perspectives for the coherent control of light fields or photochemical processes are also evoked.

PACS: 78.55.Kz, 78.55.Qr, 82.53.Xa

**Keywords**: spectral hole burning, naphthalocyanine, xerogels, two-photon absorption, spectro-temporal holography, femtosecond pulses, phase and coherent control.

## 1. Introduction

At very low temperature (4 K typical), the homogeneous spectra of an impurity molecule trapped in a solid become usually very narrow, while the inhomogeneous dispersion remains unaltered and broad. Persistent spectral hole burning (PSHB) is a method based on the use of a high selective laser source and selective photochemistry to remove the inhomogeneous broadening [1,2]. A narrow laser source tuned on the inhomogeneous band selects a sub-ensemble of isoenergetic molecules, which have coincident homogeneous absorption lines. Only the laser selected molecules are excited to their electronic state (usually the lowest one). The key point is the following: if some of the selected sites are disturbed due to a chemical or a structural photo-induced change of the guest molecule itself or of the solvent cage, then the spectra of these molecules will be modified, usually only shifted, resulting in the fact that these molecules will not absorb anymore the excitation light. As a

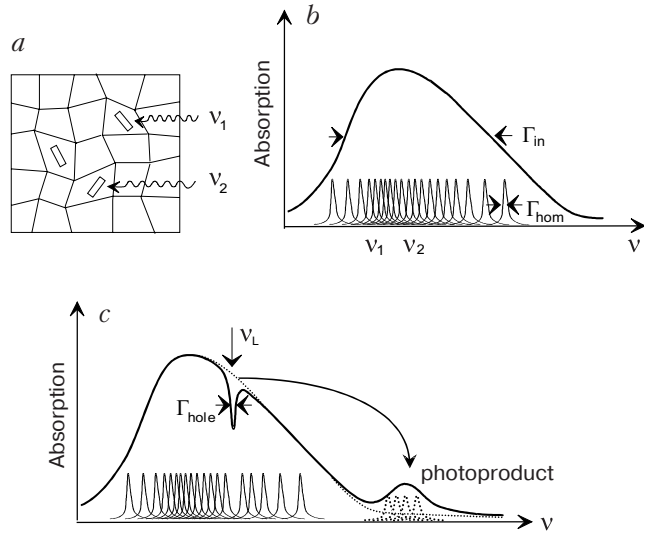


*Fig. 1.* Inhomogeneous broadening and principle of persistent spectral hole-burning.

consequence, the number of molecules with a transition frequency in resonance with the excitation light will decrease. The laser has burnt away some of the excited molecules. A dip appears in the inhomogeneous absorption band at the excitation wavelength. This dip is usually called a spectral hole (Fig. 1).

The lifetime of the spectral hole does not depend on the excited lifetime but on the mechanism, which is responsible for the change induced in the molecules or in their environment. At low temperature, the photo-induced chemical or structural change can be thermally irreversible; therefore the burnt holes will persist for quite a long time, several hours up to several years, if the system is kept at the same temperature at which the holes were produced. In that case, a hole is said persistent. A hole will be said transient if it does not last longer than a few second at the most. At first sight, the shape of a hole is Lorentzian, and in absence of saturation, the width of the hole $\Gamma_{\text{hole}}$ equals two times the homogeneous width $\Gamma_{\text{hom}}$.

$$\Gamma_{\text{hole}} = 2\Gamma_{\text{hom}}\,, \quad \Gamma_{\text{hom}} = \frac{1}{\pi T_2} = \frac{1}{2\pi T_1} + \frac{1}{\pi T_2^*}\,, \quad (1)$$

where the times $T_1$ and $T_2$ appearing in this equation are the characteristic times associated to the population relaxation $T_1$ and to the coherence or phase relaxation $T_2$.

*Why is PSHB still attractive?*

PSHB is a powerful tool to achieve high-resolution spectroscopy of complex molecules in disordered media, to study subtle photochemical events at a microscopic level in the solid state, to learn about guest-host interactions, but it can also be a powerful tool to store information data in the absorption spectra of dye-doped materials, i.e., to use the temporal frequency space or, in other words, the spectral domain. That way, PSHB allows taking advantage of the inhomogeneous broadening. Such a point of view, well connected with applications is an active research field: not only very high capacity optical memories can be imagined but, new applications in the field of image processing, real time holography, data pulse shaping and optical computation can be dreamed by combining the use of frequency selective materials with holography, short pulse techniques or electric field control. From a practical point of view, one can consider that a hole burning material behaves as a photographic plate with a very high spectral resolving power, combining in itself, the capability to store the information carried by a light wave with the spectral selectivity of a spectrometer doted with a super high resolution. To take advantage of these performances for applications — especially the very high resolution down to the sub-gigahertz range for molecular doped solids and to the kilohertz range with ion doped crystals — low temperatures down to liquid helium temperature are usually needed. Nevertheless, the interest for spectral hole burning based devices remains strong, as PSHB materials possess the attractive capability to store simultaneously spatial as well as time (spectral) information. Spectral hole burning technology is more likely to emerge in the field of optical processing because it offers outstanding performance in terms of bandwidth and time×bandwidth product. Importantly, to fix some ideas on the capabilities of PSHB materials, typical ratios between inhomogeneous and homogeneous bandwidths are in the order of $10^3$ to $10^4$ for molecular doped organic or inorganic glasses, whereas for ions doped crystals, it can reach up to $10^9$. The present review is limited to molecular doped amorphous hosts; however, we will make only one exception concerning a ion-doped crystal to explain the interest of such materials for applications in spectral analysis of radio-frequency signals in the gigahertz range with megahertz or sub-megahertz resolution.

## 2. Hole-burning

Thirty years ago, the use of laser techniques for studying dye-doped solids resulted in the development of inhomogeneous-free spectroscopies, like fluorescence line narrowing (known also as site selection spectroscopy), persistent spectral hole burning and photon-echoes techniques, applied to solid systems. Removing the influence of the spectral inhomogeneity can give access to relevant information on the guest molecule and on guest–host interactions in complex

systems. Consequently, these techniques have opened new fields of research on the dynamics of solid media at low temperatures.

Also, approximately thirty years ago, the sol-gel process that allows the insertion of organic molecules in inorganic or hybrid (organic/inorganic) matrices recovered a great interest in the research of new solid hosts for various applications in sensor, optics and electronic technologies [3]. The sol-gel process is the synthesis of an inorganic network by a chemical reaction between metal-alkoxide precursors in solution at relatively low temperatures (typically, at room temperature). The basic reaction of this process is an inorganic polymerization between silanol reactive monomers (≡Si–OH). It allows preparing glasses of new composition, which could not be obtained with ordinary high-temperature melt quenching. For instance, sol-gel materials have demonstrated their interest for solid-state laser developments [4,5], two-photon absorption induced fluorescence [6], light limiting devices or structured materials like photonic crystals [7].

In the present paper, some results obtained on dye-doped polymers and dye-doped sol-gel hosts are reviewed. A special emphasis is placed on a comparison between the two hosts. The sol-gel route to synthesize inorganic or hybrid (organic/inorganic) solid xerogels is first reminded and in what follows, a few important questions, like the problem of high-temperature PSHB materials, the search of good systems absorbing around 800 nm in view of femtosecond pulse processing and the interest of two-photon hole-burning are examined.

### *Polymers versus inorganic or hybrid (organic/inorganic) xerogels hosts*

Polymers are well known plastic solids at room temperature, easy to prepare because most of them are commercially available at any specific grade. In the literature devoted to the high-resolution spectroscopy of molecules diluted in disordered matrices at low temperatures, they represent the larger class of molecular doped systems ever studied. The advantages of polymers are: large flexibility and molecular acceptance, high optical quality in the visible range, good resistance to thermal changes and long-term stability. Their main disadvantage is that they are unable to support very intense focused light. Comparatively, the sol-gel process is known as a synthetic route for the preparation of inorganic or hybrid (organic/inorganic) glasses [8]. The first stage is a room temperature polymerization of a suitable monomer resulting in a porous and amorphous material (xerogel) in which organic molecules can be permanently trapped. For nonmolecular doped glasses, a second stage can be the closure of pores at several hundred degrees to form the final glass. The polymerization is generally initiated by adding water to a solution of an alkoxide precursor in ethanol. The tetraethoxysilane $Si(OC_2H_5)_4$ (TEOS) is one of the most used silicon alkoxide precursor. In presence of water, such alkoxide undergoes a hydrolysis reaction (I) followed by a condensation reaction leading to the formation of siloxane bridges ≡Si–O–Si≡ (II), and the process can be continued until siloxane bridges have replaced all the ethoxy groups $OC_2H_5$:

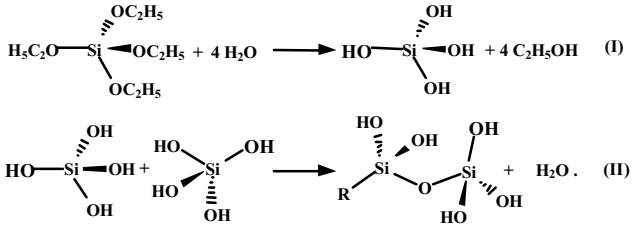


Hydrolysis and condensation initiates the formation of a silicate skeleton as a 3D-network. At that stage, a colloidal suspension in the solution is formed, which is the sol. The gelation of the sol is then caused by the percolation of clusters resulting from the aggregation phase of small-organized units. After drying in air at 20–60°C, the liquid solution is removed leading to a contraction of the gel, up to 90% in volume, and the gel turns in a dense porous material known as xerogel. Typical densities achieved after complete drying are in the order of 1.8 $g \cdot cm^{-3}$. In principle, with TEOS as the alkoxide precursor, the preparation of pure silicate xerogel should be possible. However, the reactions are never complete, leading to missing links and to the presence of residual ethoxy or hydroxyl –OH groups in the final material. Approximately, 4–5% of –OH groups remains in the matrix even after complete hydrolysis. Modifying the alkoxide precursor allows preparing hybrid xerogels mixing organic components to an inorganic silicate skeleton. For instance, the replacement of one of the ethoxy group of the TEOS molecule by an organic group R like methyl $-CH_3$ (MTEOS), vinyl $-CH{=}CH_2$ (VTEOS) or amyl $-C_5H_{11}$ (ATEOS), which does not participate in the hydrolysis–condensation reactions, has the consequence that these organic groups will stay permanently in the inorganic network:

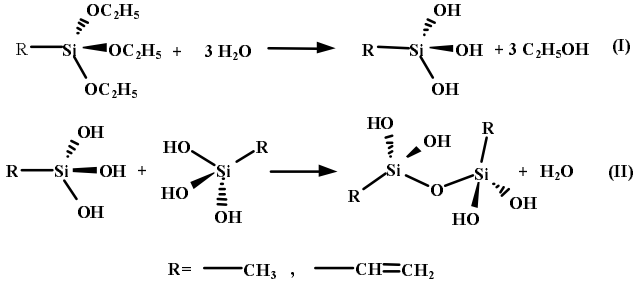

The permanent organic group R decreases the mechanical tensions during the drying process. Consequently, the final material will be closer to a plastic polymer. The softness introduced by the organic component improves its mechanical properties. Also, the decrease of the number and of the influence of the hydroxyl groups diminishes the matrix acidity, leading to an improvement of its chemical acceptance. By preparing dense xerogels with closed porosity, organic molecular species can de definitely trapped inside pores with typical sizes estimated to be in nanometer range (1–2 nm typical). The porosity (i.e., pore volume, pore size, and surface area) of materials prepared by sol-gel processing depends on the size and structure of primary sol particles formed by condensation reaction. Strategies can therefore be imagined to control the porosity of xerogels hosts. The guest interacts with the silicate matrix through an «organic carpet» whose chemical composition can be largely modified according the choice of the alkoxide precursor, and then the nature of the interaction between the guest molecule and the host can be, in some way, controlled. The presence of hydroxyl groups at the surface of the pore in pure silicate xerogels results in a relatively high acidity, which make the porous host highly chemically aggressive with most of the dopant molecules [9]. Notably, it has been revealed that one of the main reason of some spectral changes observed could be associated with the modification of the molecular structure of the impurity by means of hydrogen bonds involving the hydroxyl groups at the surface of the matrix pores [10]. Functionalized alkoxides *f*-R′-Si$(OC_2H_5)_3$, where *f* is a chemical function such as an amino or isocyanate group and R′ an alkyl spacer, allow the covalent grafting of active organic and biological molecules to the xerogel matrix [11]. The alkyl spacer limits the degrees of freedom of the grafted molecules. Other advantages are the following: limitation of the phase separation between organic molecules and the inorganic network, with an improvement of the long term chemical stability, and consequently, a possible increase of the dopant concentration at a maximum of one dopant molecule per silicon atom!

### *High-temperature persistent spectral hole burning*

Among several requirements for practical applications, high hole burning efficiencies and high-temperature persistent spectral hole burning with long-term stability are the most important. Looking for high temperatures PSHB (≥ 80 K), a good choice for the host and a good control of the coupling between the host and the guest molecule is a key point. Among the conditions that have to be fulfilled in order to burn narrow persistent spectral holes at high temperatures, two appears more important. First, the microscopic photoinduced process responsible for hole burning should give rise to a stable photoproduct. Therefore, the height of the educt-photoproduct barrier has to be high enough to preclude any possibility for a back reaction. Second, the increase of hole width and change in hole shape when rising the temperature have to be minimized.

In dye-doped solids, the electronic zero phonon line (ZPL) is accompanied by a phonon side band (PSB) on its high-energy side, which characterizes the importance of the linear electron–phonon coupling. The strength of the electron–phonon coupling is estimated via the Debye–Waller $\alpha_{DW}$ and the Huang–Rhys $S$ factors [12]. The Debye–Waller $\alpha_{DW}$ factor measures the relative importance of the ZPL contribution as compared to the PSB contribution:

$$\alpha_{DW} = \frac{A_{ZPL}}{A_{ZPL} + A_{PSB}} \qquad (2)$$

where $A_{ZPL}$ and $A_{PSB}$ are the areas of the zero phonon line and of the phonon side band, respectively. In extreme limits, for strong electron–phonon coupling, $A_{PSB}$ dominates and we have $\alpha_{DW} \approx 0$; for weak coupling, $A_{PSB}$ is near to be 0 and $\alpha_{DW} \approx 1$. The Huang–Rhys $S$ factor can be evaluated from the maximum relative hole depth measured just at the saturation limit: indeed, the saturated depth is given by $e^{-S}$ at very low temperatures, rigorously at $T$ = = 0 K [13]. Indeed, the strength of the electron–phonon coupling can be revealed easily in a PSHB experiment at long burning times when the number of molecules resonantly excited through their ZPL becomes close to be exhausted. Therefore, the hole-burning process continues with molecules excited out-of-resonance through their PSB, leading to the appearance of a *pseudo*-phonon side band growing on the red side of the zero phonon hole (ZPH). The temperature dependence of the electron–phonon coupling is another key point. In a simple model for linear electron–phonon coupling, the following temperature dependence for $\alpha_{DW}$ is predicted [14] :

$$\alpha_{DW}(\Theta) = \exp\left[-S \coth\left(\frac{\Omega_m}{2k_B\Theta}\right)\right] \qquad (3)$$

where $\Omega_m$ is the energy difference between the maximum of the PSB and the ZPL, $\Theta$ is the absolute temperature and $k_B$ is the Boltzmann's constant. From Eq. (3), it is noticeable that the decrease of $\alpha_{DW}$ when increasing the temperature will be minimum is $S$ is small and $\Omega_m$ is large. The value of $\Omega_m$ is related with the most probable energy in the phonon distribution. Consequently, guest–host systems with high-

energy phonon modes and a weak coupling strength measured by the Huang–Rhys $S$ coefficient (as low as possible) will be the most favorable for low-temperature dependence of the Debye–Waller factor $\alpha_{DW}$.

In this respect, the search was oriented in the direction of fully cross-linked 3D networks expected to have higher stiffness. Interesting attempts have been made with the studies of anionic porphyrin in polyvinylalcohol [15], tetraphenylporphin in cross-linked polymer phenoxyresin [16], dyes adsorbed on γ-alumina substrate like quinizarin or octaethylporphin [17]. Molecules encapsulated in zeolites cages have also been studied [18], as well as organic molecules inside inorganic 3D rigid silicate xerogels. The «organic carpet» can be tailored in hybrid xerogels to decrease guest–host chemical interactions and to reduce the electron–phonon coupling. However, the highest temperature at which PSHB could still be observed was never greater than 40–50 K. Higher temperatures, up to 120 K, for PSHB with organic molecules was reported for a protoporphyrin-IX grafted to alkoxysilane precursors [19]. It was conjectured that grafting the guest molecule to the host increases the rigidity of the host and limits the degrees of freedom of the dopant, reducing the contributions of molecular librations to dephasing, and consequently, to the hole width.

Exceptional PSHB performances were reported for the aluminum phthalocyanine tetrasulfonate (AlPT) hydrosoluble dye embedded in hyperquenched glassy water (HGW) [20]. HGW is an amorphous ice prepared under extreme conditions where a flow of very small (~ 1 μm diameter) droplets of water is hyperquenched under vacuum onto a cold substrate at a few kelvin. AlPT/HGW is a material whose hole-burning properties exceed, in every category, those of previously studied molecular systems. The $\Gamma_{inh}/\Gamma_{hom}$ ratio, which determines the storage density in frequency domain, has the higher value of 125 at 77 K ($10^5$ at 5 K) reported for a molecular doped solid. The burning fluence needed for the production of a zero-phonon hole with a fractional depth of 0.1 is as low as 1.5 μJ/cm$^2$. Moreover, the holes burnt in AlPT/HGW demonstrate a quite impressive resilience against destructive readout from hole burning and light-induced hole filling. For AlPT in deuterated HGW, it has been calculated that $10^8$ digital readouts could be executed before refreshing the data becomes necessary. The mechanism for hole burning of AlPT in HGW is known to be a nonphotochemical one-photon process. This result argues against the idea that only two-photon gated hole-burning materials are promising for memory/processing applications. However HGW is not a practical host medium for devices and other efficient hole burning systems with AlPT have also been reported like gelatin films [21], hydrogels i.e., polymeric hosts like water-containing poly (2-hydroxy-ethylmethacrylate) [22]. The high hole-burning efficiency is believed to be due to rearrangements occurring within hydrogen bond links formed between the hydrosoluble phthalocyanine guest and the water host. More suitable hosts that should retain the exceptional hole-burning properties of AlPT in HGW have been studied, like AlPT in a pure silicate xerogel, in a light and highly porous aerogel with large pore size and in a commercially available porous Vycor glass [12,23]. The best hole-burning performance at liquid nitrogen temperature was reported for AlPT in the porous Vycor glass in presence of water. In this system, persistent holes could be burnt in 10 s at 80 K. Measured homogeneous hole width at this temperature were about 9–10 cm$^{-1}$, to be compared to the exceptional value of 3.2 cm$^{-1}$ reported for AlPT in HGW at 77 K [20].

It is noticeable that up to date, nobody reported persistent spectral hole burning at room temperature with organic based materials.

### *In search for PSHB materials at 800 nm*

Among possible applications of PSHB, the processing of ultrashort laser pulses generated by titanium–sapphire lasers [24–26] necessitates the search for effective broadband materials exhibiting spectral hole-burning in the corresponding spectral region around 800 nm. Free-base and metallo-naphthalocyanine derivatives in polymer hosts are examples of such materials [27–29]. Studies of PSHB in silicon naphthalocyanine-doped polyvinylbutyral (PVB) with different additions of electron acceptor entities showed that, in two-color experiments, the hole-burning efficiency could be increased, especially when using fullerene $C_{70}$ additive [28,29].

In search for other molecules with a strong absorption in the 800 nm range, two stereoisomers of tetraazabacteriochlorin derivatives differing in the position of the dibenzobarrelene fragments relative to the macrocycle plane, and denoted *cis*-TABC and *trans*-TABC, have been synthesized. Absorption spectra are similar for both TABC isomers, with an intense absorption band with maximum at about 790 nm as the main feature. PSHB experiments have been reported on TABC doped PVB and silicate based xerogel hosts [30]. The spectral holes burnt in the PVB samples were much narrower than in the TEOS host (Fig. 2). Analogous facts in narrow-band PSHB-experiments at very low temperatures were interpreted as a result of a «higher degree of freedom of the guest molecules on the *surface*, as compared to molecules incorporated in

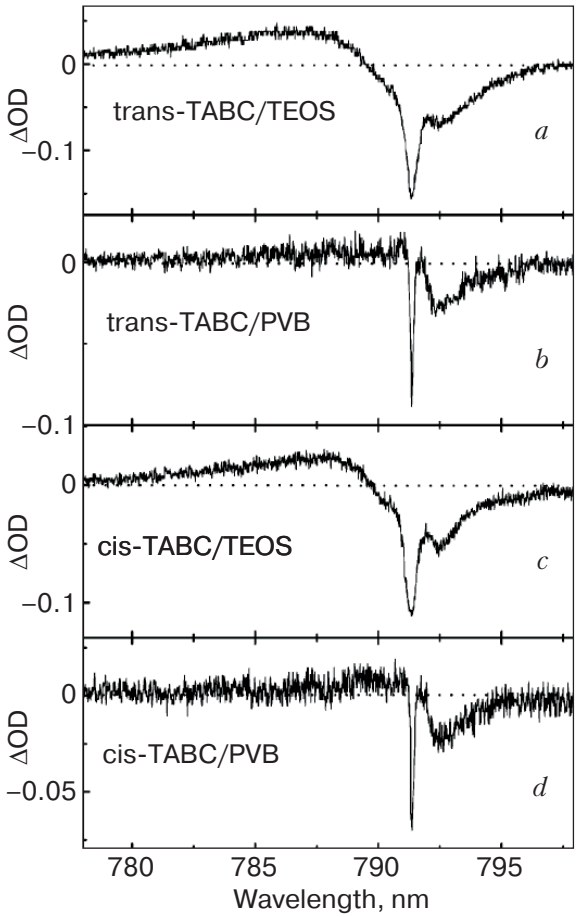


*Fig. 2*. Profiles of persistent spectral holes in the $Q_x(0,0)$ band of *trans*-TABC (*a*,*b*) and *cis*-TABC (*c*,*d*) in the PVB matrix (*b*,*d*) and TEOS xerogel (*a*,*c*). The following burning conditions have been used: Burning temperature $T_b$ = 5 K, burning wavelength $\lambda_b$ = 791.3 nm, $P_b$ = = 40 mW·cm$^{-2}$, $t_b$ = 120 s (*a*,*c*) and 180 s (*b*,*d*)).

the *bulk* of the host» [31]. The apparent hole burning efficiencies revealed by measuring the hole burning spectra with increasing the irradiation dose at the burning wavelength have been reported for *cis*-TABC doped PVB and a silicate xerogel. The hole burning efficiency was higher in the inorganic TEOS host than in PVB. This difference was assigned to the hole burning mechanism, most probably of the photochemical type in the xerogel where photoinduced changes in hydrogen bonds between the bacteriochlorin molecule and the hydroxyl −OH groups present at the surface of the pores are possible, while only nonphotochemical hole-burning can apparently play a role in PVB.

The hole-burning kinetics performances at 1.8 K have been compared between *cis*-TABC and $H_2$-T*t*BNc (tetra-*tert*-butyl naphthalocyanine) doped PVB samples. At long burning times, the hole depth achieved similar relatives values, but at short times, the kinetics at the initial stage of hole burning was definitely slower for the bacteriochlorin (rise time ~ 72 ms) that for the naphthalocyanine (rise time ~ 17 ms). Most probably the reason is a different hole-burning mechanism: in naphthalocyanine, efficient NH tautomerization should take place, while in the case of the bacteriochlorin, the NH tautomer is known to be unstable [30] and therefore does not contribute to hole burning. Consequently, this fact confirms that in the *cis*-TABC/PVB sample, the hole-burning mechanism is nonphotochemical undoubtedly related to the two-level systems (TLS) [32] flipping mechanism quite universally observed in glasses.

### *Two-photon materials*

So far, PSHB effects have been studied mostly in the case, where the ground electronic state is coupled to an excited electronic state, usually the lowest singlet one, via a resonant one-photon transition. However, an important problem for conventional PSHB systems, which use a one-photon hole-formation mechanism, is that they have serious limitation for applications due to the progressive erasing of the stored data after multiple readouts. Photon-gated PSHB [33] can achieve nondestructive reading. Two photons, usually of different colors are required in this mechanism for the photo-induced spectral change. A selective light from a narrow band laser excites a selected set of molecules within the inhomogeneous absorption band; simultaneously, a broadband source induces a photochemical event among the selected molecules. Since only the selective light is needed to record the spectral holes, no efficient photoreaction occurs during the readout step. This idea, first applied to inorganic systems, was extended to organic materials [34]. In search for new efficient photon-gated systems, especially in the 800 nm region, silicon–naphthalocyanine doped polyvinylbutyral films in the presence of electron acceptors such as citral or hexachloroethane have been studied [28]. In two-color experiments, an increase of the efficiency by a factor 10 compared with one-color results with no acceptor is achieved with green gating light, the largest increase being observed with $C_{70}$ as an acceptor. Such potentiality of $C_{70}$ fullerene to act as an optical enhancer of the hole-burning properties of Si-naphthalocyanine (SiNPc)-doped PVB films in two-color hole-burning experiments has been demonstrated [29]. Spectroscopic evidences were found that the energy initially absorbed by SiNPc molecules excited at 792 nm was transferred to $C_{70}$ fullerene molecules. This transfer is favored by the nearby low-lying and long lived triplet state of $C_{70}$ [35], allowing fullerene molecules to play a role as hole-burning activators, after their excitation with green

light to high energy states by triplet–triplet absorption.

Somewhat related to photon-gating is the two-photon absorption (TPA), which has been used earlier to demonstrate conventional, spectrally nonselective, recording in photochromic materials by focusing two perpendicularly directed laser beams [36]. This would allow actual 3D-memories with the possibility to write information in depth of a usual ~ 1-mm thick CD, increasing, in principle, its capacity ~ 1000-fold, yielding compact Terabyte (TB) carriers of information. Such an engraving in the volume of a material can be realized at room temperature because no specific high resolution spectral selectivity would be necessary, such 3D-memories using only the higher spatial resolution offered by the TPA effect. However, for high efficiency, the molecular TPA cross-section ($\sigma_2$) must be extremely large: values of $\sigma_2 > 10^4$ GM are required (1 GM = $10^{-50}$ cm$^4$·photon$^{-1}$·molecule$^{-1}$). Extending these aspects related with TPA to frequency selective photochemistry at low temperatures is of great interest as it may be also expected that using two or even three photons coherent processes instead of only one-photon transitions could use a greater variety of nonlinear effects to process optical information.

Energy-selective two-photon excitation of organic molecule was first observed [37], as well as the possibility to burn a hole by usual one-photon excitation mechanism and to detect it in TPA fluorescence excitation spectrum [38]. Also two-photon excited fluorescence line narrowing for several dyes with no inversion symmetry was demonstrated [39]. Therefore, another challenging perspective is the search for high performance two-photon hole-burning materials. In this respect, very efficient two-photon induced photo-tautomerization induced in porphyrins, chlorins and nonsymmetrical phthalocyanines has been studied [40]. It is important to notice the essential difference existing between TPA-initiated PSHB and photon-gated PSHB. A sequential absorption of two photons with the first one in resonance with the molecule absorption is implied in the latter, whereas TPA occurs via a purely virtual intermediate level. Consequently, higher energy pulses are needed for two-photon hole-burning. A typical experimental set-up is based on kilohertz repetition rate Ti:sapphire regenerative amplifier seeded by a mode-locked Ti:sapphire femtosecond oscillator. For exciting organic molecules such as porphyrins, typically used for SHB experiments, infrared pulses are needed. Therefore, an optical parametric amplifier (OPA) is used to convert the 780 nm pulses into near infrared pulses tunable in the range 1100–1800 nm [41]. It has been demonstrated that a multiphoton, sum-frequency type process, rather than conventional one-photon process can create coherence at high illumination intensity, in an inhomogeneously broadened organic dye-doped polymer medium. Two-photon spectral gratings can be detected through spontaneous fluorescence or persistent spectral hole-burning at long exposure times. The temperature dependence of the Debye–Waller factor and the phonon spectrum of two-photon transition was obtained in presence of large inhomogeneous broadening [41]. The wavelength dependence of absolute two-photon absorption cross section in a series of octaethyl-, tetraphenyl-, and tetrabenzo-substituted porphyrins established that the TPA efficiency of porphyrins in 710–810 nm region is resonantly enhanced due to nearby Q(0–0) one-photon transition [42].

### 3. Spatio-temporal holography

Using photochemically accumulated photon echoes [43] in a PSHB material, one engraves a sinusoidal grating in temporal frequency space with the two first pulses delayed by $\tau$. Later, a third pulse is diffracted on the engraved grating, giving rise to the echo in a well-defined direction [44]. By using noncollinear delayed pulses, a sinusoidal spatial grating and a sinusoidal spectral grating are engraved in the ma-

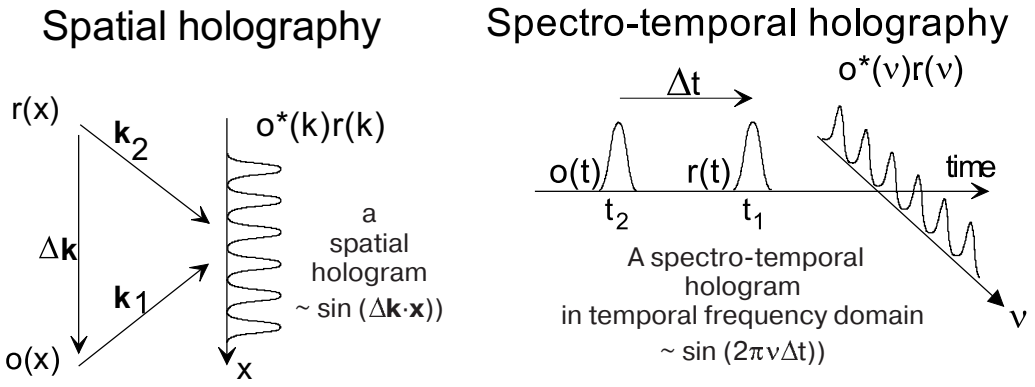


*Fig. 3*. Analogy between spatial and spectro-temporal holography.

terial. Notice that the spectral hologram can be engraved alone by using collinear pulses, only delayed by $\tau$. The sinusoidal spectral grating is the simplest spectral hologram, in the same way as the spatial grating is the simplest spatial hologram, as represented in Fig. 3.

Evidently, a hologram can be much richer than a simple grating. As holography demonstrated that 3D scenes could be stored in a spatial hologram, «temporal images» can be stored in a spectral hologram. This is the essence of spectro-temporal holography for which spectrally selective materials are the most appropriate. Combining the experimental configuration of conventional spatial holography with spectral holography in frequency selective hole-burning materials, one realizes the form of spatial-spectro-temporal-holography the more complete, capable to map not only the spatial distribution of an electromagnetic field, but also to memorize its time evolution in the absorption spectrum.

*Engraving the electric field of a light wave*

For the engraving of a conventional hologram, a point $\mathbf{r}$ of a photosensitive material is illuminated by an object $a(\mathbf{r})$ and a reference $b(\mathbf{r})$ monochromatic fields, which interfere at that point i.e., the received intensity is equal to $[a(\mathbf{r}) + b(\mathbf{r})]^2$. Therefore, the engraving at that point is proportional to the product $a(\mathbf{r})\cdot b^*(\mathbf{r})$ and the signal resulting from the diffraction at this point of a readout field $c(\mathbf{r})$ is proportional to the triple product $a(\mathbf{r})\cdot b^*(\mathbf{r})\cdot c(\mathbf{r})$. It is noticeable that the emitted signal at the point $\mathbf{r}$ is only a function of the engraving at this point, and then reflecting its local character in the spatial domain. With conventional photosensitive materials (a photographic plate, a photorefractive crystal), this locality is not in the temporal frequency space, which means that a hologram engraved with the green light of an argon ion laser can be readout with the red light of a helium-neon laser.

The situation is different with a frequency selective material. In this case, the locality can be also present in the temporal frequency domain, meaning that, to define an engraved point, its spatial coordinates $\mathbf{r}$ have to be completed with its temporal frequency $\nu$. Consequently, by using polychromatic fields characterized by the amplitudes $\tilde{a}(\mathbf{r},\nu)$, $\tilde{b}(\mathbf{r},\nu)$ and $\tilde{c}(\mathbf{r},\nu)$ defined in each point $(\mathbf{r},\nu)$, the engraving at the point $(\mathbf{r},\nu)$ is proportional to the product $\tilde{a}(\mathbf{r},\nu)\cdot\tilde{b}^*(\mathbf{r},\nu)$ and the contribution from this spatio-spectral point to the holographic signal is given by:

$$\tilde{s}(\mathbf{r},\nu) = \tilde{a}(\mathbf{r},\nu)\cdot\tilde{b}^*(\mathbf{r},\nu)\cdot\tilde{c}(\mathbf{r},\nu) \qquad (4)$$

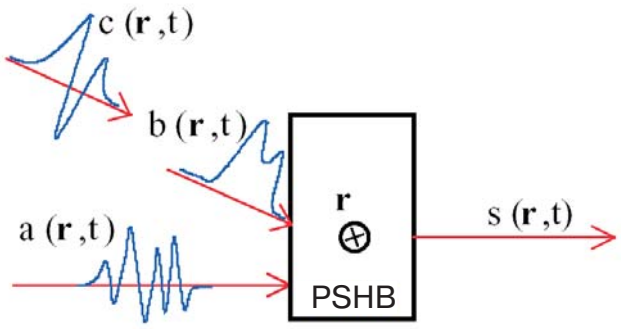


*Fig. 4.* The most general case of the spatial and spectral interference of polychromatic pulses with arbitrary temporal shapes. First, a spectral–spatial–temporal hologram is engraved by pulses $b(\mathbf{r},t)$ and $a(\mathbf{r},t)$; note that pulse $b$ arrives first. The temporal response $s(\mathbf{r},t)$ to the probe pulse $c(\mathbf{r},t)$ is given by a double convolution containing the conjugate form of the pulse $b$: $b^*(\mathbf{r},t)$.

which means that the spectral component at the frequency $\nu$ of the probing signal is diffracted by the component of the hologram at the same frequency and by this one only (Fig. 4).

The spectral and temporal amplitudes of the light fields, $\tilde{f}(\mathbf{r},\nu)$ and $f(\mathbf{r},t)$, are conjugated by Fourier transform according the equation:

$$f(\mathbf{r},t) = \int d\nu \tilde{f}(\mathbf{r},\nu)\ \exp\,(2i\pi\nu t). \qquad (5)$$

Substituting this relation in Eq. (4), the temporal amplitude of the signal is then:

$$s(\mathbf{r},t) = a(\mathbf{r},t) \otimes b(\mathbf{r},-t) \otimes c(\mathbf{r},t) \qquad (6)$$

where $\otimes$ represents the convolution of the temporal profiles of the light waves. Notice that in Eq. (6), the evolution of the $b$ field appears time reversed. These complicated mathematical treatment are realized quasi-instantaneously in a PSHB material with spatially and temporally structured fields. In this fruitful approach, the light wave fields, which can have complicated spatial and temporal shapes, are directly manipulated. With the use of the preceding equation, different experimental arrangements can be considered with the aim of performing different optical processes.

Quite easy simplifications are obtained by using simple light field profiles. For example, an ultrashort pulse (a delta Dirac's pulse) of a plane wave i.e., $b(\mathbf{r},t) = b\delta(t)$, will have a constant profile in the spectral domain, solving in a simplistic way the convolution operation. Optical data storage in a PSHB memory and retrieval of the stored data can be performed using a configuration where the reference pulse $b(\mathbf{r},t)$ strikes on the sample first. In these conditions, the echo signal $s(\mathbf{r},t) = TF\,[\tilde{a}(\mathbf{r},\nu)] =$

$= a(\mathbf{r},t)$ reproduces identically the object $a(\mathbf{r},t)$ pulse. A different situation is realized if the object $a(\mathbf{r},t)$ arrives on the sample before the reference $b(\mathbf{r},t)$ pulse. At the reading stage with the probe $c(\mathbf{r},t)$ pulse, the echo signal $s(\mathbf{r},t) = TF\,[\tilde{a}^*(\mathbf{r},\nu)] = a(\mathbf{r},-t)$ is the time reversed object $a(\mathbf{r},t)$ pulse. Finally, a third situation can be considered, which corresponds to the case of temporal pattern recognition. For this, the reading pulse is no more a Dirac's pulse but a pulse, which can be identical to the object pulse or different. Therefore, the signal being $s(\mathbf{r},t) = TF\,[\tilde{a}(\mathbf{r},\nu)\cdot\tilde{c}(\mathbf{r},\nu)] = a(\mathbf{r},t) \otimes c(\mathbf{r},t)$ will be equal to *one* if $c(\mathbf{r},t) \equiv a(\mathbf{r},t)$ or equal to *zero* if $c(\mathbf{r},t) \neq a(\mathbf{r},t)$.

In the following paragraph, we demonstrate the retrieving of a chirped pulse or of its time-reversed replica using naphthalocyanine-doped polyvinylbutyral as a PSHB memory. From this experiment, we have proposed the application of PSHB materials in a new method for the temporal aberration free recompression of stretched pulses.

### *Ultrafast pulse shaping*

Ultrashort laser pulses have revolutionized the field of laser-matter interaction. Since the development of titanium–sapphire femtosecond laser source, the domain of research fields or development covered by the use of ultrafast lasers is in continuous expansion, from high-energy physics to ultrafast chemistry (femtochemistry) and new microscopy techniques. For a given spectral width, the shortest pulse is the pulse, which is Fourier transform of the spectrum. A Fourier transform pulse has no frequency chirp, and then great efforts in ultrashort laser pulse technology have been deployed to eliminate any frequency chirp. It was also realized that, when in a photochemical reaction for example different pathways lead to a given final state, the presence of a well-controlled frequency chirp might greatly enhance the probability with which this final state is reached [45]. In both cases, chirp control is needed and mastering the phase of the laser pulse is the key point.

Usual techniques for producing high-energy ultrashort pulses use the chirped pulse amplification (CPA) scheme, in which a combination of gratings and reflective optics to realize the stretching, amplification and compression stages are employed [46]. The direct amplification of ultrashort pulses would produce instantaneous peak power at a power that expensive parts of the chain could be destroyed. In a CPA chain (Fig. 5), the amplification of femtosecond pulses is realized trough a three stages combination. First, the Fourier transform femtosecond pulse is stretched up to several picoseconds, and then it is amplified up to thousand times and finally re-compressed to femtoseconds. In such a chain, basically the stretcher and the compressor are completely symmetrical dispersive devices. For a perfect recompression, mastering the pulse evolution is the key point. In a CPA chain, the compressor must fully correct the phase changes introduced by the stretcher and the amplifier. Indeed, they are not aberration free systems and the aberrations they introduced, as well as the aberrations introduced by the amplifier itself are not compensated. At the output, the amplified pulses need then to be cleaned in accordance with their future use. Some passive schemes help to eliminate a part of the geometric aberrations, however most of these corrections are not sufficient to eliminate phase distortions of high order that are due to the presence of a large amount of material in the laser chain and to the surface quality of the reflective optical elements used in the stretcher.

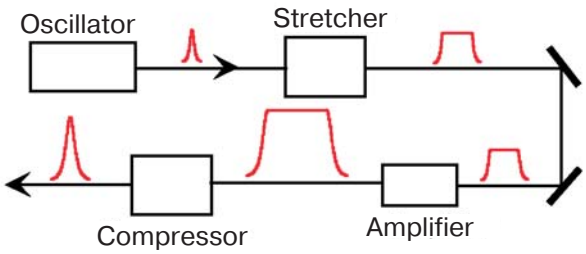


*Fig. 5.* Scheme of a chirped pulse amplification chain. The pulse delivered by the oscillator is first stretched, then amplified and finally recompressed. A stretcher (or a compressor) is a dispersive device which introduces a linear chirp $d\phi/dt = \mu(\omega-\omega_0)$, resulting in a quadratic phase in the spectral domain $\phi = \frac{1}{2}(\omega-\omega_0)^2$.

For better compression, active correction of the temporal profiles of high-intensity pulses with liquid-crystal spatial light modulators [47], deformable mirrors [48], acousto-optic modulators [49] has been demonstrated. For instance, spectral phase corrections can be achieved with the help of a two grating zero dispersion line in the Fourier plane of which a liquid crystal array is inserted [50], however the spectral resolution and the pixelization of the spatial light modulator in the Fourier plane are the most crucial limitations of this shaping technique.

As explained previously, the temporal image of a pulse object field may be spectrally stored in the PSHB material. Therefore, to realize the perfect aberration free recompression of previously stretched pulses, a different approach based on the use of a PSHB material in which the conjugate of the transfer function of the compressor and amplifier stages can be engraved in the spectral domain has been proposed (Fig. 6). At the retrieving stage, a time conjugate of the chirped pulse, which passed through the comp-

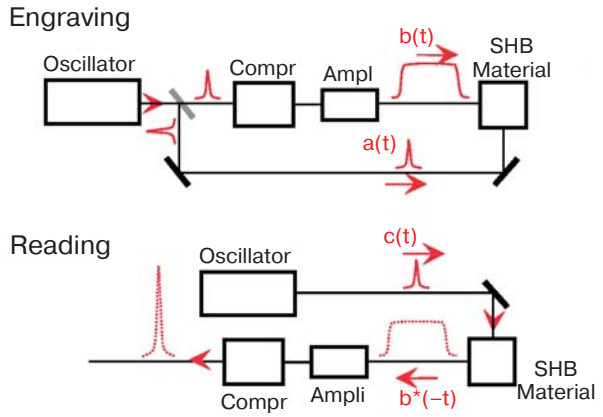


*Fig. 6*. An alternative scheme for chirped pulse amplification based on a PSHB material. Two steps are required: at the programming stage, a coherent filter is engraved with a chirped pulse and a reference pulse. At the reading stage, a temporally phase conjugated replica of the chirped pulse is generated and further amplification and compression result in an aberration free amplified pulse. It is mandatory that the same amplifier and stretcher be used in both stages.

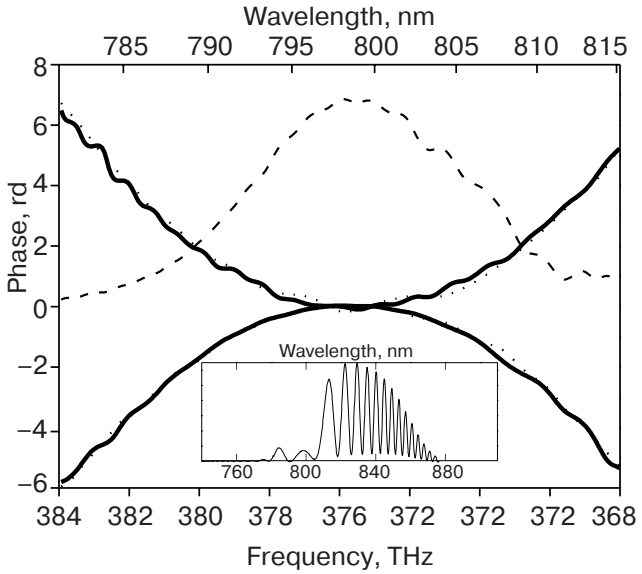


*Fig. 7*. Demonstration of the phase control of femtosecond chirped pulses. Solid lines: spectral phase of the diffracted pulse for two delays $\tau$ and $-\tau$ between the writing pulses. Thin dotted lines: spectral phase difference between the 2 writing pulses for the two cases $\tau$ and $-\tau$. The thin dashed line represents the spectral amplitude of the diffracted pulse. Inset: spectral interference fringes between the unchirped and chirped writing pulses at time delay equal 0 at 800 nm. The chirp is formed by propagation through a SF58 glass plate of thickness 1.7 cm.

ressor and the amplifier, is emitted. By passing it through the amplifier and the compressor again, it is amplified and re-compressed, with the phase aberrations automatically compensated.

Modifying the phase of an ultrashort laser pulse or correcting a phase change implies that one is able to measure this phase. The spectral interferometry (SI) technique [51] that perfectly suits ultrashort pulses is expected to be the ideal tool. A reference pulse is sent through the device, and the output pulse and a portion of the incident reference pulse are made to frequency beat on the entrance slit of a spectrometer. The resulting spectrogram provides the required information [52]. The control of the phase of femtosecond pulses shaped using spectral holography in a PSHB material was demonstrated [53,54]. Spectral interferometry was used for measuring the amplitude and phase of photon echo signals produced by diffraction of femtosecond pulses on a spectral hologram engraved in a free base naphthalocyanine doped polyvinylbutyral ($H_2$NPc/PVB) sample. A chirp was introduced on one of the two pulses used for engraving by a 1.7 cm thick SF58 glass plate and the spectral interference between the chirped and a reference unchirped pulse was engraved in the absorption band. In this experiment, the diffracted pulse (the echo) was collinear with the incident pulse but delayed by $\tau$.

Time reversal was easily achieved by changing the time ordering between the two writing pulses, i.e., the time delay is changed from $+\tau$ to $-\tau$ and the object pulse is sent before the other writing pulse. The recovered spectral phase is then observed to be the opposite of that obtained in the previous case (Fig. 7).

At low temperatures, the expected spectral resolution which could be achieved by burning spectral holes in a molecular doped solid is in the sub-gigahertz range. Therefore, the engraving and the retrieving of spectral structures using pulses separated by nanosecond delays should be in principle feasible. However, one limitation in using SI with long delays is the limited resolving power of the spectrometer. To overcome this problem, an experiment was made in a noncollinear geometry and using a second delay line placed in between the cryostat and the spectrometer used for the analysis by spectral interferometry. This second delay line compensated the delay between the echo signal and the probe pulse in such a way that the detection of the spectral interferometry signal was always close to the zero delay. This arrangement allowed the best use of the limited spectral resolution of the spectrometer. Examples of some recorded signals are shown in the Fig. 8.

The passage of one of the pulses through a dispersive stretcher line with two gratings chirped the pulse. At 2 K, it was observed that the echo could be easily retrieved even for a long delay of about 1 ns. These results demonstrate the possible use of the full

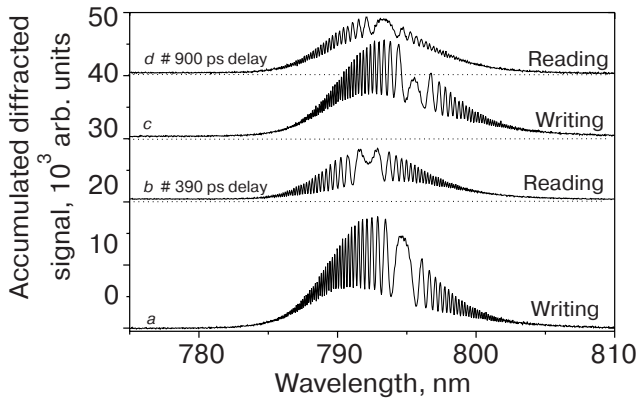


*Fig. 8.* Examples of retrieved echo signals analyzed using the spectral interferometry technique. Typical conditions for writing were: $P_b \sim 5$ mW for «reference» and «object» beams, $t_b \sim 60$ s. Beams were non-focused ($\phi \sim 2$ mm). One of the pulses was stretched and chirped by passing through a two-grating dispersive line. In this experiment, the probe pulse was identical to the «object» one and attenuated by passing through an OD = 3.6 filter for reading. The introduction of this OD filter was responsible for the shift of the «zero chirp» position.

storage capabilities of naphthalocyanine-doped material in femtosecond experiments [55].

### *Coherent control of ultrafast pulses*

The use of optimally shaped pulses to control the temporal evolution of a system is a challenging research field. The flexibility offered by the manipulation of the interacting light in the coherent control of quantum systems has been realized since the middle of the 1980's years [56] and it has been demonstrated [57] for both simple and complex systems such as atoms, molecules, and semiconductors (for a review see [16]). For instance, a coherent control experiment has proved that the spectral profile of the exciting pulse determines the rate of a two-photon absorption process [58] or the yield of a photodissociation reaction [59]. Pulse shaping efficiently accelerated the rotation of a diatomic molecule, climbing up the ladder of rotational states as the frequency content of the laser pulse constantly changed to match the changing Raman transition energy [60].

Two main approaches have been attempted in coherent control experiments. The first one is based on an open-loop scheme, which consists in reaching a specific goal without any experimental feedback. The second one uses a closed-loop scheme in which a feedback control is sent to a pulse shaper device for optimizing the response of the system. Algorithms for feedback control are using genetic or evolution rules [61] and they are adapted to program a computer-controlled pulse shaper based on a two grating zero dispersion line. An adaptive algorithm begins by initializing a random population of pulse shapes. These pulses interact with the molecular system. The most efficient ones according a predefined goal are selected, slightly modified and a new population of pulse shapes is generated for a new cycle. The adaptive process is continued until no more evolution is needed. Despite the great success of this approach, inconveniences of conventional pulse shaper devices can be found in their limited spectral resolution and their pixelized structure for some of them.

PSHB molecular doped solids allow a different approach to femtosecond pulse shaping where they combine the roles usually played by the dispersive components and the modulator arrays [62]. A PSHB material is nonpixelated and potentially offers a larger number of addressable points. As usual with PSHB material, the temporal image of a pulse object field can be spectrally stored, and the shaping process includes two steps: first, engraving a coherent spectral filter with an accumulated storage interferometric procedure, followed with the use of this filter to shape a probe pulse. If the latter pulse is the same as the (short) reference pulse of the engraving process, the «diffracted» or echo pulse reproduces the object pulse or its time-inverted image, depending on the pulse time ordering. Similarly to spatial phase conjugation that leads to self-compensation of spatial phase distortions, the stimulated photon echo technique may lead to spectral phase conjugation i.e., time reversal provided that, because of causality, the reference pulse follows (rather than precedes) the object pulse [63]. With the use of PSHB materials, an important remark has to be made: since the relevant spectral information is stored as population changes, the engraving process does not require ultrashort pulses and «almost any» temporal shape may be programmed and stored, and later retrieved using a short reading pulse.

Coherent control of quantum systems may require a more complex phase and amplitude shaping, and for this purpose PSHB materials have the required qualities. The programming of the material can be performed with properly tailored pulse sequences. In principle, it is possible at the engraving stage, to substitute the preparation pulses, pulse 1 and 2 of the three pulses of the echo sequence, by writing a frequency dependent modulation into the inhomogeneously broadened absorption line of a PSHB burning material with a cw laser controlled both in intensity and frequency. By directly programming the hole-burning material, any echo temporal shape should be generated. Persistent hole-burning materials could be suitably programmed for coherent control of a process in an open-loop scheme, while transient hole-burning could possibly be used in closed-loop scheme.

The first spectrally programmed stimulated photon echo was obtained using a cryogenic $Eu^{3+}$:$YAlO_3$ sample with a quasi-persistent hole lifetime exposed to a frequency-scanned and intensity-modulated cw laser for multiple hole-burning. At the reading stage, a coherent burst equivalent to the stimulated photon echo was obtained by triggering this sample by a pulsed laser. That was the first demonstration that any desired transient pulse shape could, in principle, be obtained by appropriate frequency-domain programming, modulating artificially the inhomogeneous distribution of a medium [64]. Other demonstration experiments were performed using ion doped inorganic materials, mainly for the reason that cw laser sources are more easily scanned over a limited frequency range. The use of broadband PSHB molecular doped solids is much more problematic. The use of broadband spectrally selective materials for coherent control appears as a challenging prospect. May be, it is no so unrealistic to imagine the use of molecular doped solids for the coherent control of processes in atoms or ions. Therefore, it should be possible to take benefit of the higher spectral resolution offered by a liquid helium cooled dye-doped host spectrally programmed over a limited frequency range. Combining transient hole burning, «box-car» writing and reading scheme, fast tuning of a cw laser source and continuously refreshed programming should be possible, allowing the realization of closed-loop control.

## 5. Conclusion: the material issue

Furthermore than the issue of the need for low temperatures, the other problem for the use of optical storage devices in spectral domain based on frequency selective doped solids is the difficulty to synthesize suitable materials with all the best performances at the same time. Two main material families are considered according the application domain considered. For instance, rare earth ions doped crystals have inhomogeneous bandwidth in the range of 1 to 100 GHz, with homogeneous widths from 0.1 to 100 kHz at 2 K (giving a typical $\Gamma_{inh}/\Gamma_{hom}$ ratio of about $10^6$ to $10^8$). These bandwidths are perfectly tuned for a coupling with electronic devices, and these materials are well adapted for high performances optoelectronic applications. Their advantages are demonstrated through the realization of the spectral analysis of broadband radio-frequency signals [65,66]. Conversely, molecular doped polymers and molecular doped xerogels with inhomogeneous bandwidths in the THz range ($\Gamma_{inh}$ ~ a few nm = 5 to 15 THz typical) and homogeneous widths of about 0.1 to 10 GHz at 4 K ($\Gamma_{inh}/\Gamma_{hom}$ ratio of about $10^3$ to $10^4$) are suitable for «all-optical» applications where large bandwidths, far away electronic devices can manage, are needed. They match very well the qualities of commercially available light sources. Table 1 summarizes and compares the main characteristics of both materials with conventional optics performances.

Among the problems to solve for applications of persistent spectral hole-burning to optical memory and processing technologies are the finding of efficient hole-burning materials, with high storage density in the frequency domain, resilience against destructive readout and operation at high temperatures (77 K). To date, the search for the good material, which combines all the favorable properties, is still a challenging task. The most important performances needed for applications are summarized in the Table 2 below. The table mainly takes into account molecular doped solid and briefly indicates some materials, which have the best response to the considered property.

In the present review, polymers and sol-gel hosts have been compared in respect to several important properties and capabilities in view of their potentialities to be used in practical devices. These comparative studies have demonstrated that molecular doped polymers and molecular doped xerogels have similar hole-burning behavior. However, in considering the control of the electron–phonon coupling contribution or the hole-burning performances at high temperature, inorganic hosts based on silicate xerogels

Table 1. A comparison in the spectral domain between the characteristics of materials and the performances of optical devices.

| System ⇒ / Characteristics ⇓ | Molecular doped polymers or xerogels | Ion doped crystals | Conventional optics WDM |
|---|---|---|---|
| Inhomogeneous width ( = bandpass) | 10 THz | 10–100 GHz | > 100 THz |
| Homogenous width ( = channel width) | 100 MHz–1 GHz | 100 Hz–100 kHz | 100 GHz |
| Time×Bandpass product ( = number of channels) | $10^3$–$10^5$ | $10^6$–$10^9$ | $10^2$–$10^3$ |

Table 2. Needed requirements for spectral hole-burning materials in view of possible applications.

| Needed performance | Materials |
|---|---|
| $\Gamma_{hole}$ = 100-500 MHz, $\Gamma_{inh}/\Gamma_{hom}$ high (>$10^3$, $10^4$) | Chlorin/PVB, OEP/PS, AlPT/HGW, colour centres |
| Usable at diode laser frequencies $\lambda$ = 830 nm, $\lambda$ = 640 nm or even shorter | $H_2Pc/H_2SO_4$, $H_2NPc$/PVB, R′ centres in LiF, $Tm^{3+}$/YAG (793 nm) |
| Usable at telecom laser frequencies $\lambda$ = 1.3 μm or $\lambda$ = 1.5 μm | $Er^{3+}/Y_2SiO_5$ |
| Reversibility | $H_2P$, $H_2Pc$, colour centres |
| Long lifetime persistence of holes at low temperature | Quinizarin/alcohol glasses |
| High hole-burning efficiency (30 ns/bit) | $(tBu)_4H_2Pc$/PE, |
| Photon gated hole-burning mechanism | $Sm^{2+}$/BaClF, TZT/$CHCl_3$/PMMA, carbazole/BA, perylene/BA |
| Thermo-resistant holes | $Sm^{2+}$/BaClF, hydrophenazin/fluorene, NV centres in diamond |
| Room temperature hole-burning | $Sm^{2+}$/BaClF, $Eu^{3+}/Al_2O_3$-$SiO_2$ glasses |
| Thin film technology compatibility | Colour centre clusters, polymer thin films |

$H_2P$: free-base porphyrin, $H_2Pc$: free-base phthalocyanine, $H_2NPc$: free-base naphthalocyanine, OEP: octaethylporphyrin, AlPT: aluminum phthalocyanine tetrasulfonate, $(tBu)_4H_2Pc$: tetra-tert-butylphthalocyanine, TZT: meso-tetra(*p*-tolyl)-Zn-tetrabenzoporphyrin, BA: boric acid, HGW: hyperquenched glassy water, PE: polyethylene, PS: polystyrene, PMMA: polymethylmethacrylate, PVB: polyvinylbutyral.

or porous glasses have shown the best results. Importantly also, grafting the active molecule to the host has allowed a great improvement in terms of high-temperature hole burning. However these experiments needs strong efforts for synthesizing suitable precursor molecules, and consequently there is quite few exploitable results. Of course, the use of inorganic matrices is not always possible due to the acidic properties of these hosts, which can strongly interact with the guest and modify its chemical structure and properties. However, the sol-gel synthesis, which allows combining inorganic and organic properties is far to have been fully explored and therefore the hope is still strong that converging efforts from chemists, photochemists, physicists, theoreticians and engineers, one can largely improves the performances of these molecular doped solids.

In the development of the present paper, examples of possible applications based on the use of molecular doped solids at liquid-helium temperature, which should allow to achieve ultrafast performance on time scale of $10^{-12}$–$10^{-13}$ s, as these materials enable SHB recording and coherent transient responses with broad optical bandwidth of 5–10 THz [67] were given. For these demonstrations, systems with sufficiently high efficiencies (>$10^{-2}$) have to be used. In principle, the resilience to successive multiple readouts can be substantially increased with the use of photon-gated hole-burning materials. A quite challenging problem is to find systems in which persistent and narrow stable holes can be burnt at temperatures as high as possible. Not only this problem is of interest for applications purposes, but it also focus the attention on the delicate problem of how to control the coupling between the host and a guest molecule.

The research field for challenging systems with absorption band around 800 nm and optimized PSHB properties is of great interest. In future prospect, the use of optimally shaped pulses to control the temporal evolution of a system is another challenging research field. The demonstration of the phase control of chirped pulse using frequency selective hole-burning materials was made and that the aberration free recompression of stretched pulses can be performed. PSHB materials can be used as programmable filters for pulse shaping, with application to the coherent control of quantum systems. Coherent control may require a more complex phase and amplitude shaping, for which it was demonstrated that PSHB materials have the required qualities. It is in principle possible at the engraving stage, to substitute the preparation pulses by the writing of a frequency dependent modulation into the inhomogeneously broadened absorption line of a PSHB material with a cw laser controlled both in intensity and frequency. Consequently, by directly programming the hole-burning material, any echo temporal shape should be generated. The use of broadband spectrally selective PSHB materials for coherent control appears as a challenging prospect, however, besides the material issue, the most important problem to solve should be the realization of highly reliable cw laser sources rapidly tunable over a few nanometer wavelength ranges.

In finishing this paper, I would like to thank all of them who have collaborated to the collection of results summarized here, concerning the studies on

PSHB materials: A.-V. Veret-Lemarinier, S. Kulikov, S. Arabei, J. Rice, S. Leach, N. Landraud, F. Chaput, J.-P. Boilot and for the spectro-temporal holography: J.-L. Le Gouet, M. Joffre, J.-P. Likforman, S. Fraigne, and A. Gorokhovsky.

1. W.E. Moerner (ed.), *Persistent Spectral Hole Burning: Science and Applications*, *Topics in Current Physics*, Springer–Verlag (1988).
2. J.-P. Galaup, *Spectral Selective Studies of Molecular Doped Solids and Applications*, in: *Advances in Multiphoton Processes and Spectroscopy*, Vol. 16, World Scientific Publishing Co Pte Ltd, Singapore (2004), p. 77.
3. D. Levy, S. Einhorn, and D. Avnir, *J. Non-Cryst. Solids* **113**, 137 (1989).
4. M. Canva, P. Georges, J.-F. Perelgritz, A. Brun, F. Chaput, and J.-P Boilot, *Appl. Opt*. **34**, 428 (1995).
5. D. Lo, S.K. Lam, C. Ye, and K.S. Lam, *Opt. Commun*. **156**, 316 (1998).
6. M. Canva, G. Roger, F. Cassagne, Y. Levy, A. Brun, F. Chaput, J.-P. Boilot, A. Rappaport, C. Heerdt, and M. Bass, *Opt. Materials* **18**, 391 (2002).
7. O.J.A. Schueller, G.M. Whitesides, J.A. Rogers, M. Meier, and A. Dodabalapur, *Appl. Opt*. **38**, 5799 (1999).
8. C.J. Brinker and G.W. Scherer, *Sol-gel Science, the Physics and Chemistry of the Sol-gel Processing*, Academic Press, London (1990).
9. S.G. Kulikov, A.-V. Veret-Lemarinier, J.-P. Galaup, F. Chaput, and J.-P. Boilot, *Chem. Phys*. **216**, 147 (1997).
10. S.M. Arabei, J.-P. Galaup, T.A. Pavich, and K.N. Solovyov, *J. Lumin*. **94-95**, 767 (2000).
11. J.-P. Boilot, F. Chaput, J.-P. Galaup, A.-V. Veret-Lemarinier, D. Riehl, and Y. Levy, *Special Ceramics Processing Issue*, *AIChE J*. **43**, 2820 (1997).
12. J.-P. Galaup, S. Fraigne, N. Landraud, F. Chaput, and J.-P. Boilot, *J. Lumin*. **98**, 189 (2002).
13. W.H. Kim, T. Reinot, J.M. Hayes, and G.J. Small, *J. Phys. Chem.* **99**, 7300 (1995).
14. K.K. Rebane and I. Rebane, *J. Lumin*. **56**, 39 (1993).
15. K. Sakoda, K. Kominami, and M. Iwamoto, *Jpn. J. Appl. Phys.* **27**, L1304 (1988).
16. K. Horie, T. Mori, T. Naito, and I. Mita, *Appl. Phys. Lett*. **53**, 935 (1988); A. Furusawa, K. Horie, K. Kukori, and I. Mita, *J. Appl. Phys*. **66**, 6041 (1989).
17. T. Basché and C. Bräuchle, *J. Phys. Chem.* **95**, 7130 (1991); B. Sauter and C. Brauchle, *Chem. Phys. Lett.* **192**, 321 (1992).
18. M. Ehrl, F.W. Deeg, C. Bräuchle, O. Franke, A. Sobbi, G. Schulz-Ekloff, and D. Wohrle, *J. Phys. Chem.* **98**, 47 (1994).
19. A.-V. Veret-Lemarinier, J.-P Galaup, A. Ranger, F. Chaput, and J.-P. Boilot, *J. Lumin*. **64**, 223 (1995).
20. W.H. Kim, T. Reinot, J.M. Hayes, and G.J. Small, *J. Phys. Chem.* **99**, 7300 (1995); T. Reinot, W.H. Kim, J.M. Hayes, and G.J. Small, *J. Chem. Phys*. **104**, 793 (1996); T. Reinot, J.M. Hayes, and G.J. Small, *J. Chem. Phys*. **106**, 457 (1997).
21. T. Reinot, W.H. Kim, J.M. Hayes, and G.J. Small, *J. Opt. Soc. Am.* **B14**, 602 (1997).
22. J.M. Hayes, T. Reinot, and G.J. Small, *Chem. Phys. Lett.* **312**, 362 (1999).
23. J.-P. Galaup, S. Fraigne, N. Landraud, F. Chaput, and J.-P. Boilot, *J. Lumin*. **94-95**, 719 (2001).
24. T. Chanelière, S. Fraigne, J.-P. Galaup, M. Joffre, J.-L. Le Gouet, J.-P. Likforman, and D. Ricard, *European Phys. J. - Applied Physics* **20**, 205 (2002).
25. S. Fraigne, J.-P. Galaup, J.-L. Le Gouet, B. Bousquet, L. Canioni, M. Joffre, and J.-P. Likforman, *J. Opt. Soc. Am.* **B20**, 1555 (2003).
26. J.-P. Galaup, S. Fraigne, J.-L. Le Gouet, J.-P. Likforman, and M. Joffre, *J. Lumin*. **107**, 187 (2004).
27. A.V. Turukhin, A.A. Gorokhovsky, C. Moser, I.V. Solomin, and D. Psaltis, *J. Lumin*. **86**, 399 (2000).
28. S. Fraigne, J.H. Rice, and J.-P. Galaup, *J. Lumin*. **94-95**, 649 (2001).
29. S. Fraigne and J.-P. Galaup, *J. Lumin*. **98**, 231 (2002).
30. J.-P. Galaup, S.M. Arabei, K.N. Solovyov, T.A. Pavich, and E.A. Makarova, *J. Phys. Chem.* **A108**, 9510 (2004).
31. J.D. Keegan, A.M. Stolzenberg, Y.C. Lu, R.E. Linder, G. Barth, A. Moscowitz, E. Bunnenberg, and C. Djerassi, *J. Am. Chem. Soc.* **104**, 4305 (1982).
32. W.A. Phillips, *J. Low Temp. Phys.* **7,** 351 (1972); P.W. Anderson, B.I. Halperin, and C.M. Warma, *Philos. Mag*. **25**, 1 (1972); W.A. Phillips, *Rep. Prog. Phys.* **50**, 1657 (1987).
33. A. Winnacker, R.M. Shelby, and R.M. Macfarlane, *Opt. Lett.* **10**, 350 (1985).
34. H.W.H. Lee, M. Gehrtz, E.E. Marinero, and W.E. Moerner, *Chem. Phys. Lett.* **118**, 611 (1985); T.P. Carter, C. Braüchle, V.Y. Lee, M. Manavi, and W.E. Moerner, *J. Phys. Chem.* **91**, 3998 (1987); R.M. Macfarlane, *J. Lumin*. **38**, 20 (1987); H. Suzuki and T. Shimada, *Mol. Cryst. Liq. Cryst.* **217**, 165 (1992); S. Salhi, S.G. Koulikov, C. Bied-Charreton, and J.-P. Galaup, *J. Lumin*. **78**, 187 (1998).
35. J.H. Rice, J.-P. Galaup, and S. Leach, *Chem. Phys*. **279**, 23 (2002).
36. D.A. Parthenopoulos and P.M. Rentzepis, *Science* **245,** 843 (1989).
37. M.F. Granville, G.R. Holtom, B.E. Kohler, R.L. Christensen, and K.L. D'Amico, *J. Chem. Phys*. **70**, 593 (1979).
38. M.C. Edelson, J.M. Hayes, and G.J. Small, *Chem. Phys. Lett.* **60**, 307 (1979).
39. M. Takeda, K. Matsuda, C. Suzuki, and S. Saikan, *J. Lumin*. **86**, 285 (2000).
40. M. Drobizhev, C. Sigel, and A. Rebane, *J. Lumin*. **86**, 391 (2000); M. Drobizhev, A. Karotki, and A. Rebane, *Chem. Phys. Lett.* **334**, 76 (2001); M. Kruk, A. Karotki, M. Drobizhev, V. Kuzmitsky, V. Gael, and A. Rebane, *J. Lumin*. **105**, 45 (2003).

41. A. Rebane, M. Drobizhev, and A. Karotki, *J. Lumin.* **98**, 341 (2002).
42. M. Drobizhev, A. Karotki, M. Kruk, and A. Rebane, *Chem. Phys. Lett.* **355**, 175 (2002).
43. W.H. Hesselink and D.A. Wiersma, *Phys. Rev. Lett.* **43**, 1991 (1979).
44. D.A. Wiersma and K. Duppen, *Science* **237**, 1147 (1987).
45. M. Shapiro and P. Brumer, *J. Chem. Phys.* **84**, 4103 (1986); P Brumer and M. Shapiro, *Chem. Phys. Lett.* **126**, 541 (1986).
46. D. Strickland and G. Mourou, *Opt. Commun.* **56**, 219 (1985).
47. A. Efimov and D.H. Reitze, *Opt. Lett.* **23**, 1612 (1998).
48. E. Zeek, K. Maginnis, S. Backus, U. Russek, M. Murnane, G. Mourou, H. Kapteyn, and G. Vdovin, *Opt. Lett.* **24**, 493 (1999); G. Chériaux, O. Albert, V. Wänman, J.-P. Chambaret, C. Félix, and G. Mourou, *Opt. Lett.* **26**, 169 (2001).
49. F. Verluise, V. Laude, Z. Cheng, C. Spielmann, and P. Tournois, *Opt. Lett.* **25**, 575 (2000).
50. C. Froehly, B. Colombeau, and M. Vampouille, in: *Progress in Optics*, E. Wolf (ed.), North-Holland, Amsterdam (1983), Vol. **20**, p. 65; A.M. Weiner, *Rev. Sci. Instrum.* **71**, 1929 (2000).
51. C. Froehly, A. Lacourt, and J.C. Vienot, *Nouv. Rev. Opt.* **4**, 183 (1973) (*in French*).
52. L. Lepetit, G. Cheriaux, and M. Joffre, *J. Opt. Soc. Am.* **B12**, 2467 (1995); M.F. Emde, W.P. de Boeij, M.S. Pshenichnikov, and D.W. Wiersma, *Opt. Lett.* **22**, 1338 (1997).
53. S. Fraigne, J.-P. Galaup, J.-L. Le Gouët, B. Bousquet, L. Canioni, M. Joffre, and J.-P. Likforman, *J. Opt. Soc. Am.* **B20**, 1555 (2003).
54. J.-P. Galaup, S. Fraigne, J.-L. Le Gouët, J.-P. Likforman, and M. Joffre, *J. Lumin.* **107**, 187 (2004).
55. J.-P. Galaup and A. Gorokhovsky, accepted, *J. Lumin.* (2007).
56. D.J. Tannor and S.A. Rice, *J. Chem. Phys.* **830**, 5013 (1985); M. Shapiro and P. Brumer, *J. Chem. Phys.* **84**, 4103 (1986); D.J. Tannor, R. Kosloff, and S.A. Rice, *J. Chem. Phys.* **85**, 5805 (1986); W.S. Warren, H. Rabitz, and M. Dahleh, *Science* **259**, 1581 (1993).
57. S.A. Rice, *Science* **258**, 412 (1992); E.D. Potter, J.L. Herek, S. Pedersen, Q. Liu, and A.H. Zewail, *Nature* (London) **355**, 66 (1992); B. Kohler, V.V. Yakovlev, J. Che, J.L. Krause, M. Messina, K.R. Wilson, N. Schwentner, R.M. Whitnell, and Y. Yan, *Phys. Rev. Lett.* **74**, 3360 (1995); A. Haché, Y. Kostoulas, R. Atanasov, J.L.P. Hughes, J.E. Sipe, and H.M. van Driel, *Phys. Rev. Lett.* **78**, 306 (1997); R.N. Zare, *Science* **279**, 1875 (1998); D.C. Clary, *Science* **279**, 1879 (1998).
58. D. Meshulach and Y. Silberberg, *Nature* (London) **396**, 239 (1998); D. Meshulach and Y. Silberberg, *Phys. Rev.* **A60**, 1287 (1999).
59. A. Assion, T. Baumert, M. Bergt, T. Brixner, B. Kiefer, V. Seyfried, M. Strehle, and G. Gerber, *Science* **282**, 919 (1998).
60. D.M. Villeneuve, S.A. Aseyev, P. Dietrich, M. Spanner, M.Y. Ivanov, and P.B. Corkum, *Phys. Rev. Lett.* **85**, 542 (2000).
61. T. Baumert, T. Brixner, V. Seyfried, M. Strehle, and G. Gerber, *Appl. Phys.* **B65**, 779 (1997); B.J. Pearson, J.L. White, T.C. Weinacht, and P.H. Bucksbaum, *Phys. Rev.* **A63**, 063412 (2001).
62. M. Mitsunaga, R. Yano, and N. Uesugi, *Opt. Lett.* **16**, 264 (1991); H. Schwoerer, D. Erni, A. Rebane, and U.P. Wild, *Opt. Commun.* **107**, 123 (1994).
63. T.W. Mossberg, *Opt. Lett.* **7**, 77 (1982).
64. M. Mitsunaga, R. Yano, and N. Uesugi, *Opt. Lett.* **16**, 264 (1991).
65. J.-P. Galaup, F. Grelet, J.-L. Le Gouët, D. Dolfi, and J.-P. Huignard, *Analyseur de Spectre de Frequence*, French Patent, INPI Registration n°: FR9802626, registration date: March 4, 1998, INPI Publication n°: FR2775790, date of publication: September 9, (1999); L. Menager, I. Lorgere, J.-L. Le Gouet, D. Dolfi, and J.-P.Huignard, *Opt. Lett.* **26**, 1245 (2001).
66. G. Gorju, V. Crozatier, I. Lorgeré, J.-L. Le Gouët, and F. Bretenaker, *IEEE PTL* **17**, 2385 (2005); F. Schlottau, M. Colice, K.H. Wagner, and W.R. Babbitt, *Opt. Lett.* **30**, 3003 (2005).
67. A. Rebane, *SPIE Proc.* **3468**, 270 (1998).